FERMILAB-PUB-77-119-E
MSU-CSL-38

DIMUON AND TRIMUON FINAL STATES IN DEEP INELASTIC MUON SCATTERING*

C. Chang and K. Wendell Chen

Michigan State University

East Lansing, Michigan 48824

and

A. Van Ginneken

Fermi National Accelerator Laboratory, Batavia, Illinois 60510

ABSTRACT

Thirty-two dimuon and eleven trimuon events are observed in deep inelastic muon interactions at 150 GeV. The rate of dimuon production is greater than 5×10^{-4} that of inclusive muon scattering. High inelasticity trimuons occur at a rate one order of magnitude lower. These events are more numerous and the extra muons have qualitatively different production characteristics than muons expected from conventional sources. The data suggest the production and subsequent decays of heavy particles.

* Work supported in part by the National Science Foundation under Grant No. GP29070 and by the U.S. Energy Research and Development Administration.

Multimuon events are observed[1] in a data sample of a previous experiment on deep inelastic muon-nucleon interactions at 150 GeV.[2,3] Production rates and characteristics are inconsistent with either π and K decays or low mass quantum electrodynamical (QED) tridents being the source of these muons. Assuming production of "direct" muons by virtual photons to be similar to that observed in hadron-hadron interactions leads to prediction too low by two orders of magnitude.

Processes yielding one extra muon (2μ) in the final state ($\mu N \to \mu\mu X$) are observed to occur at a rate slightly larger than 5×10^{-4} per deep inelastic muon scattering event. The acceptance of the apparatus is approximately such that the muons must have an energy larger than about 17 GeV and an angle larger than about 13 mrad. In addition the events should not be accompanied by a penetrating charged particle at an angle less than 13 mrad. Events with three muons (3μ) in the final state ($\mu N \to \mu\mu\mu X$) are found to occur at a rate roughly about 10^{-4} per deep inelastic muon scattering event. This Letter deals mostly with 2μ events. Analysis of trimuon events will appear separately.

The apparatus (Fig. 1) consists of a 194 cm (1.57×10^3 g/cm^2) long iron-and-scintillator target followed by three (79 cm long, 173 cm diameter) toroidal iron magnets, interspersed by an array of wire-spark chambers. In the central core of the toroidal magnets (at radii less than 15.2 cm) the iron is replaced by lead-loaded concrete and the magnetic field effectively vanishes in this region. Likewise at radii below 15.2 cm there is an inactive region in the spark chambers. Two beam veto counters (30.5 cm in diameter) placed before and after the last magnet reject those events with a penetrating charged particle at a small angle. More detail about the apparatus is given in Refs. 1-3.

The present data sample derives from a total of 6.8×10^9 incident muons of 150 GeV. The trigger requirement is for a muon to penetrate all three toroidal magnets and register in each spark chamber. This corresponds roughly to the energy and angle cuts mentioned above. In the exposure 25,550 single μ events are thus registered. The scanning criteria to search for multimuon events are: 1) the muon trajectories (both scattered and produced muons) extrapolate to the beam track to within 2 cm; 2) triggering muon and the accompanying muon(s) can be momentum analyzed by at least one magnet; 3) correct timing and hodoscope information is observed for all final state muons; and 4) the origin of the events must lie within the iron target. A total of 32 2μ's and 11 3μ's are observed in this manner. Most 2μ events were accompanied by a shower which extends at least through 20 cm of iron as seen by the iron-scintillator target array.

The observed origin of the multimuons is uniform along the beam direction in the target. This uniformity discriminates against the possibility that these events are due to the small pion contamination of the muon beam (about 10^{-5} π per μ). Independently of the argument a calculation based on 150 GeV pion induced dimuon data[4] shows this component to have an upper limit of about 1% of the observed 2μ event rate. Likewise the charge structure (see below) is inconsistent with a large fraction of the 2μ events being of hadronic origin.

The 43 multimuon events are divided according to charge distribution as follows: 1) for μ^+ incident: 10 $\mu^+\mu^-$, 10 $\mu^+\mu^+$, 4 $\mu^+\mu^+\mu^-$; 2) for μ^- incident: 5 $\mu^-\mu^+$, 7 $\mu^-\mu^-$ and $7\mu^-\mu^-\mu^+$. In 2μ events of opposite charge the energy of the scattered muon E_{μ_1} is unambiguously determined and is found to exceed the energy of the produced muon E_{μ_2} in each event. This feature is used to identify the scattered and produced muon in pairs of the same charge. The results are shown in Fig. 2. For all 2μ events $\langle E_{\mu_1} \rangle / \langle E_{\mu_2} \rangle = 2.8$. When μ^+ and μ^-

incident events are combined the produced μ in 2μ events appears to be equally likely of either charge. The charge structure of 3μ events is consistent with produced muon pairs being always of opposite charge.

The assumption which identifies the leading muon as the scattered muon defines the mass and momentum of the virtual photon. In contrast with neutrino scattering experiments the standard kinematical variables associated with the muon scattering vertex are here readily obtained: $y = \nu/E_\mu$, $q^2 = 4E_\mu E_{\mu_1} \sin^2(\theta/2)$, $x = q^2/2M\nu$ and $W^2 = M^2 + 2M\nu - q^2$ where E_μ is the incident muon energy, $\nu = E_\mu - E_{\mu_1}$, M is the nucleon mass and θ is the scattering angle. Fig. 3 (a-d) shows the distribution of the 2μ events for each of the variables defined above. Three 2μ events are not shown in the graphs due to an ambiguity in E_{μ_1} measurement. In Fig. 4 (a) and (b) are shown respectively the (integrated) energy distribution of the produced μ and the transverse momentum measured with respect to the virtual photon direction.

Summarizing the most striking features of the 2μ events as exhibited by the raw data: (1) $E_{\mu_1} > E_{\mu_2}$ in opposite sign pairs; (2) no charge preference of the produced muon; (3) apparent threshold in the invariant mass W; (4) "flat" p_T distribution up to 2.6 GeV/c, $dN/dp_T \sim \exp(-2p_T)$; (5) no observed peak in the apparent mass; (6) $\langle x \rangle_{2\mu} = 0.05$ versus $\langle x \rangle_{1\mu} = 0.11$; (7) $\langle q^2 \rangle_{2\mu} = 7.5$ (GeV/c)^2 versus $\langle q^2 \rangle_{1\mu} = 15.0$ (GeV/c)^2; and (8) copious hadron production as seen in the iron-scintillator target array.

The multimuon events are unlikely due to π or K decays. This is indicated by the expected low p_T values of decay muons and the small acceptance of the apparatus at low p_T. A Monte Carlo calculation confirms this. The target-detector geometry and magnetic field are included in fairly detailed manner. The muon-nucleus interaction is simulated using experimentally measured inclusive hadron production distributions[5] at 150 GeV and a charged hadron

multiplicity (W and q^2 dependent) from lower energy electroproduction.[6] Kaon production is assumed to follow the same inclusive distribution as for pions but with 1/10th of the multiplicity. The particles produced in the initial interaction are allowed to interact further in the target and produce more secondary hadrons. This cascade process is continued through the entire apparatus down to sufficiently low energy of the participating particles.[7] The scattered muon as well as the decay muons are likewise traced through the apparatus.

The hadrons participating in the cascade shower are expected to produce "prompt" muons, and this component has been evaluated using fits of single μ production of protons on nuclei at 200 GeV/c and below.[4] Likewise the virtual photon can be expected to produce prompt muons from conventional sources (e.g. vector mesons). To estimate this component it is assumed that such prompt muons and pions are produced in the same ratio as observed in hadron-hadron collisions. (To the extent that prompt μ's are emitted pairwise their contributions are overestimated).

Background muons from electromagnetic tridents can be produced both coherently and incoherently via a Bethe-Heitler, bremsstrahlung or deep Compton production process.[8] The detection apparatus is biased severely against QED processes which occurs mostly at low four-momentum transfers of the virtual photon or muon propagators. In addition, to be observed as 2μ events, one of the trident members must escape detection either due to its low energy or due to an excessively large angle of emmission ($\theta_2 \geq 200$ mrad). In a separate Monte-Carlo calculation, the 2μ yield from QED tridents surviving the experimental cuts is calculated.[9] The background calculations are summarized in Fig. 4. Other processes may be expected to contribute at a far lower rate: QED events from μe scattering, muon production via Lee-Wick bosons, intermediate vector bosons[10] or Bethe-Heitler heavy lepton pairs.[11] The total back-

ground discussed here is about 4.9 events. Therefore most multimuon final states do not appear to come from readily identifiable sources.

The abundance of dimuons and trimuons as well as the kinematic distributions strongly suggest the production and decay of heavy particles produced in deep inelastic muon interactions.[1,12] It should be noted that the measurement of the production cross section of heavy particles permits the evaluation of the contribution to deviations from Bjorken scaling at $x < 0.1$. However, it is presently far from clear whether this could explain all of the observed scale-breaking effects in deep inelastic muon scattering.[2,3,13]

The net total of 27 dimuon events yield a cross section--uncorrected for acceptance--of 5×10^{-36} cm^2/nucleon for the process $\mu N \rightarrow \mu\mu X$. Requiring the fastest dimuon member to be the triggering particle provides the uncorrected rates of 2μ production relative to the number of observed single muon events: $\sigma(\mu N \rightarrow \mu\mu X)/\sigma(\mu N \rightarrow \mu X) = 5 \times 10^{-4}$. The above values as well as the various distributions presented here are strongly dependent of the acceptance of the apparatus. The present results can be extrapolated to predict the total cross section and the distributions in terms of the various kinematical variables only by assuming a definite muon production model.[14] Our analysis of the data based on associated production of charmed hadrons (as well as other hypothetical particles produced at the leptonic vertex) and their subsequent decay in the apparatus will appear elsewhere. By comparing the corrected dimuon and trimuon rates an estimate of the muonic branching ratio of these produced particles is possible, at least in principle.

To further investigate multimuon production a high statistics experiment at $E_\mu = 275$ GeV has recently been completed at Fermilab. This experiment provides a 50-fold increase in luminosity as well as a substantial reduction in energy and angle thresholds.[15]

It is a pleasure to acknowledge the assistance of the staff of Fermilab during the data-taking phase. We thank A. Kotlewski, L. Litt, L. Hand, S. Loken, M. Strovink and W. Vernon for their early contributions to this work.

REFERENCES

1. K. W. Chen, in Proceedings of the International Conference on New Particles with New Quantum Numbers, (University of Wisconsin, Madison, 1976).
2. Y. Watanabe et. al, Phys. Rev. Lett. 35, 898 (1975).
3. C. Chang et. al, Phys. Rev. Lett. 35, 901 (1975).
4. K. J. Anderson et. al, Phys. Rev. Lett. 36, 237 (1976); ibid. Phys. Rev. Lett. 37, 799 (1976); J. G. Branson, et. al, Phys. Rev. Lett. 38, 457 (1977).
5. W. A. Loomis et. al, Phys. Rev. Lett. 35, 1483 (1975). The expression of the inclusive distribution cited for $0<x'<1$ is used. For $1<x'<0$, an expression that fits the lower energy electroproduction data is used.
6. P. H. Garbincius et. al, Phys. Rev. Lett. 32, 328 (1974).
7. A. Van Ginneken, FNAL Report No. FN-272, 1975, (unpublished).
8. S. Brodsky and S. Ting, Phys. Rev. 145, 1018 (1966); P. Kessler, Acta Physica, Austriana 41, 141 (1975); Nuovo Cimento 53, 809 (1960).
9. The calculation of QED tridents includes coherent and incoherent elastic contributions. The total cross section for other QED processes is much smaller while differences in acceptance are highly unlikely to promote their contribution to a large fraction of the observed total, cfr. C. Carimalo et. al, Phys. Rev. D10, 1561 (1974). We thank S. Brodsky for providing us with his trident program.
10. R. W. Brown and J. Smith, Phys. Rev. D3, 207 (1971); R. Linsker, Phys. Rev. D5, 1709 (197_); H. Fearing, M. Pratap and J. Smith, Phys. Rev. D5, 158, (1972).
11. Y. S. Tsai, Rev. Mod. Phys. 46, 813 (1974). The possibility of heavy lepton production at the muonic vertex is not considered here.

12. A. De Rujula, in Proceedings of the 1976 Coral Gables Conference, Miami, Florida, 1976; S. L. Glashow, in Proceedings of the International Conference on New Particles with New Quantum Numbers, (University of Wisconsin, Madison, 1976); J. Pati and A. Salam, Trieste Preprint IC/76/63 (1976); F. Bletzacher, H. T. Nieh and A. Soni, Phys. Rev. Lett. 37, 1313 (1976); V. Barger and R. J. N. Phillips, Phys. Rev. Lett. 65B, 167 (1976); S. Nandi and H. Schneider, Bonn preprint HE-76-24, (1976); L. Baulieu and C. Piketty, LPTENS preprint 76/16 (1976); D. P. Roy, Tata Institute preprint, (1977); H. D. Politzer, Harvard Preprint, HUTP-77/A001 (1977).

13. H. Anderson et. al, in Proceedings of the XVIII Conference in High Energy Physics, Tbilisi, USSR, 1976.

14. For example, without a detailed knowledge of the apparatus, Barger and Phillips (Ref. 11) estimate on the basis of a charm production model, that the corrected rate for $\sigma(2\mu)/\sigma(1\mu)$ is 0.5×10^{-2}.

15. Experiment 319, Fermilab, Michigan State-Fermilab Collaboration.

Figure Captions

Fig. 1. Layout of apparatus. P denotes proportional chambers, S spark chambers, T trigger counters, and V veto counters.

Fig. 2. Scatter plot of the energy of the members of a dimuon of opposite sign (left) and of same sign (right). Circles correspond to incident μ^+, triangles to incident μ^-. The lines $E_1 = nE_2$ are drawn to guide the eye.

Fig. 3. Histograms of single muon and dimuon events.

(a) invariant recoil mass, W

(b) fractional energy of virtual photon, y

(c) scaling variable x and

(d) 4-momentum transfer squared, q^2.

Fig. 4. (a) Integral energy spectrum of the slowest dimuon member (number of events with $E_{\mu 2} > E$).

(b) Transverse momentum distribution relative to the virtual photon direction of the slowest dimuon member. Various background components are shown: decay μ from π and K in the hadronic cascade following the μ interaction (I), prompt μ from the initial interaction via conventional processes (II), prompt muons produced by the hadronic cascade (III), QED tridents with one muon undetected (IV), and total background (V). Errors shown are statistical errors only.

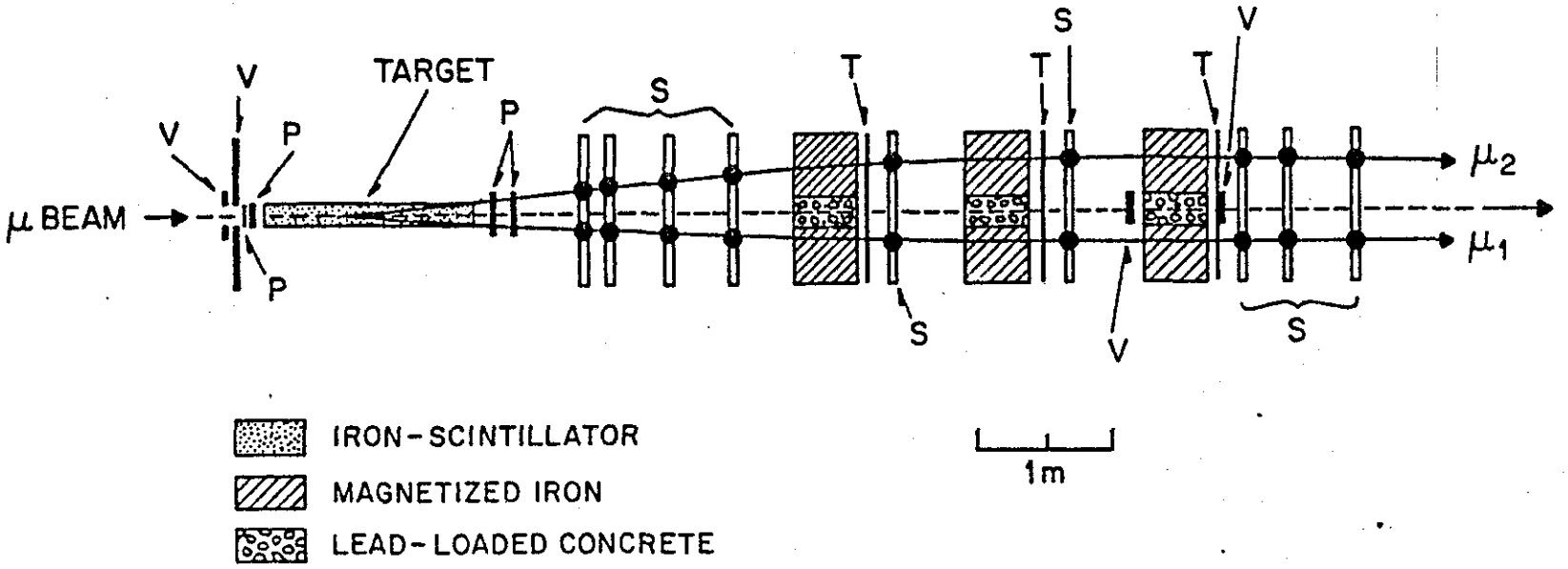
μ BEAM
V
V
P
P
TARGET
P
S
T
T
S
T
V
S
V
μ2
μ1
IRON-SCINTILLATOR
MAGNETIZED IRON
LEAD-LOADED CONCRETE
1m

FIGURE 1

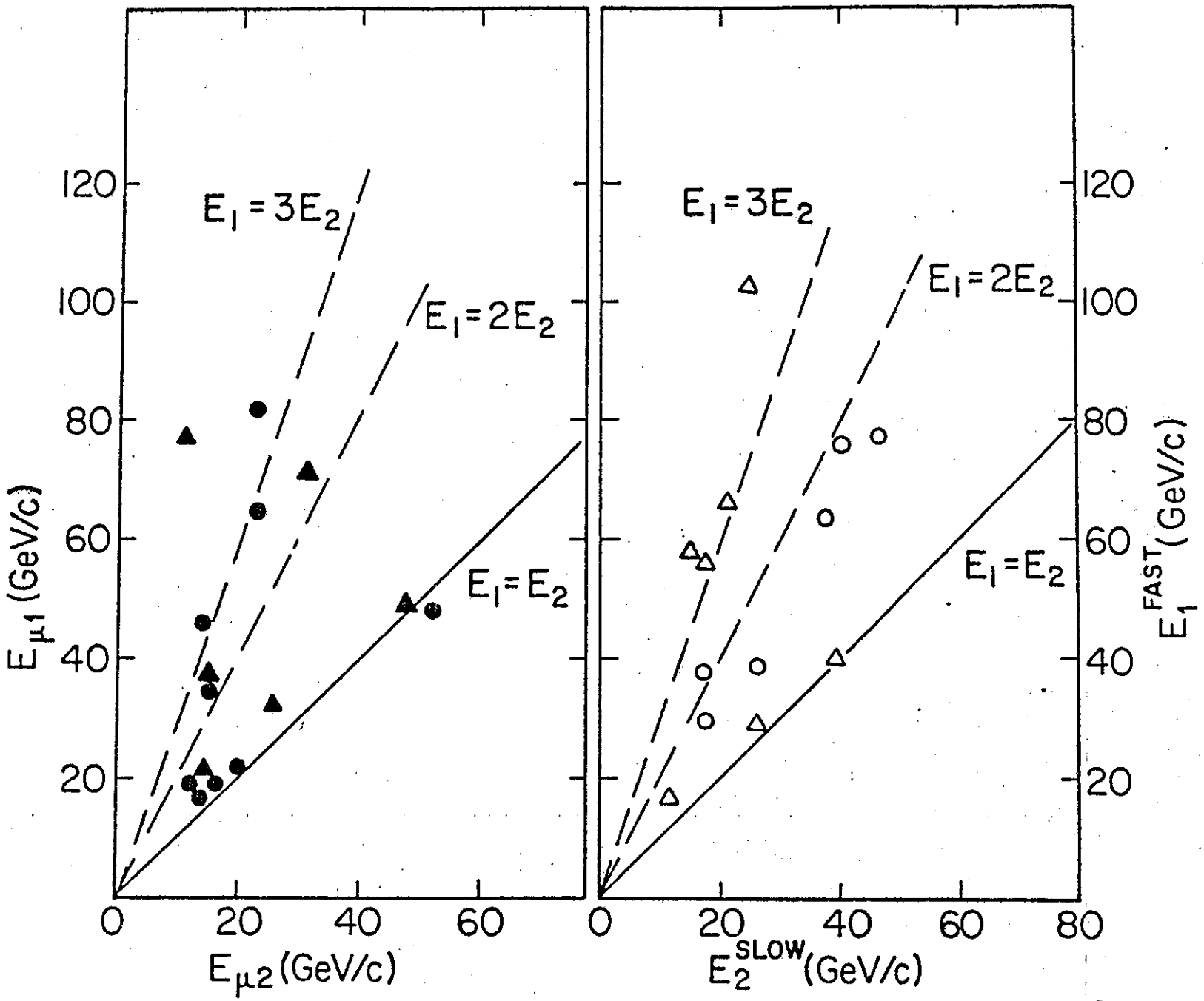
$E_1 = 3E_2$
$E_1 = 2E_2$
$E_1 = E_2$
$E_{\mu 1}$ (GeV/c)
$E_{\mu 2}$ (GeV/c)
E_1^{FAST} (GeV/c)
E_2^{SLOW} (GeV/c)
0
20
40
60
80
100
120

FIGURE 2

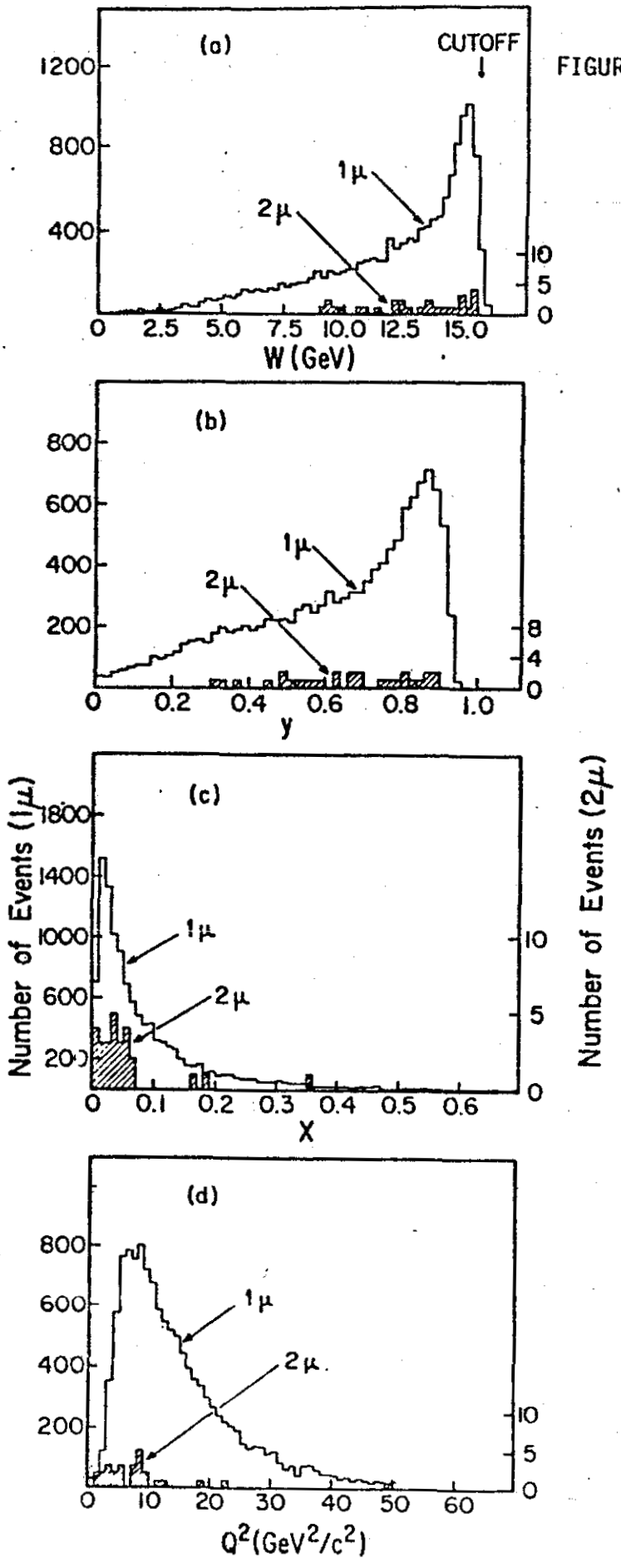
(a)
CUTOFF
1200
800
400
1μ
2μ
10
5
0
0 2.5 5.0 7.5 10.0 12.5 15.0
W (GeV)
(b)
800
600
400
200
1μ
2μ
8
4
0
0 0.2 0.4 0.6 0.8 1.0
y
(c)
Number of Events (1μ)
1800
1400
1000
600
200
1μ
2μ
10
5
0
Number of Events (2μ)
0 0.1 0.2 0.3 0.4 0.5 0.6
X
(d)
800
600
400
200
1μ
2μ
10
5
0
0 10 20 30 40 50 60
Q² (GeV²/c²)

FIGURE 3

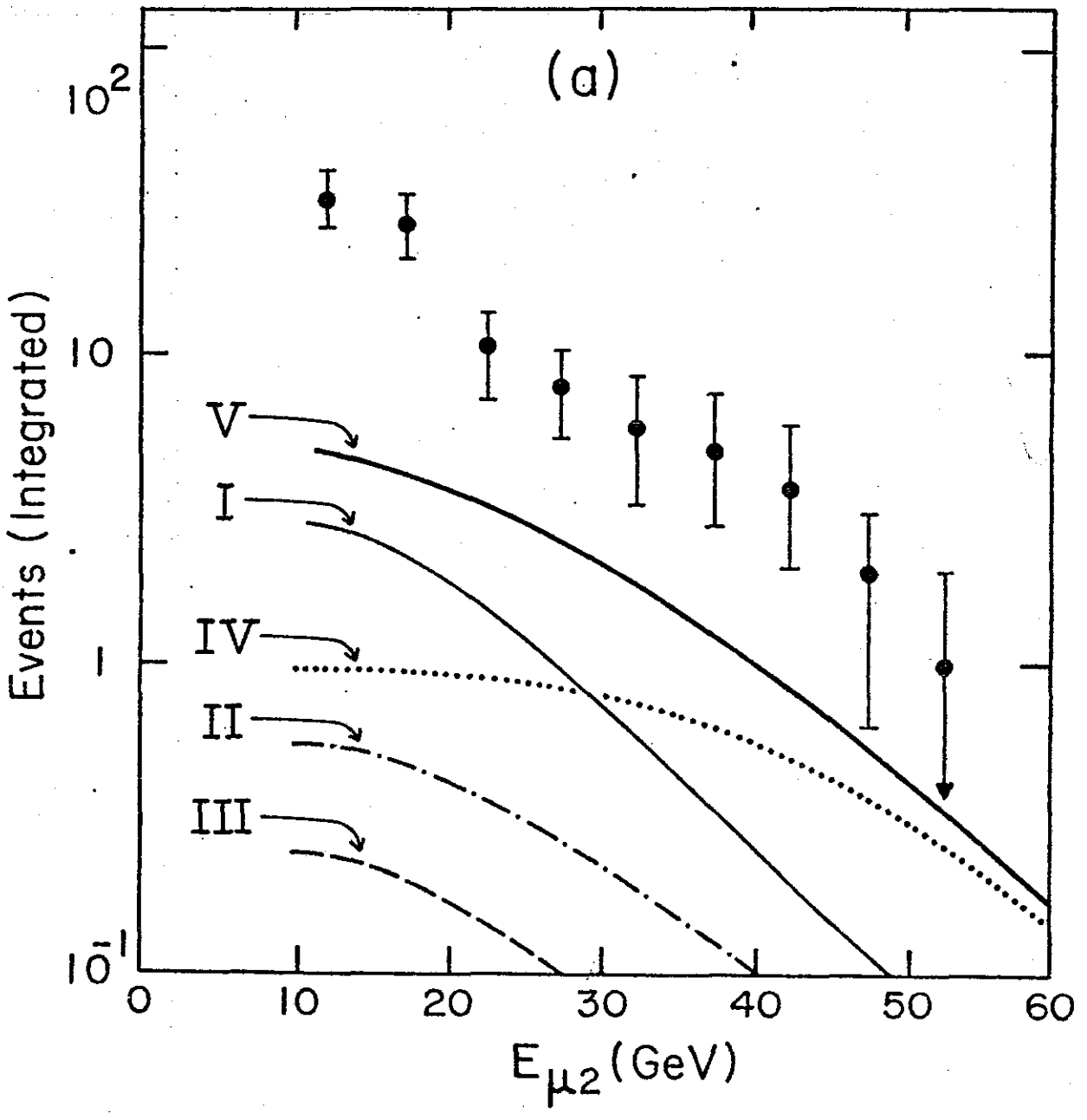
(a)
10^2
10
1
10^{-1}
Events (Integrated)
V
I
IV
II
III
0
10
20
30
40
50
60
$E_{\mu 2}$ (GeV)

FIGURE 4(a)

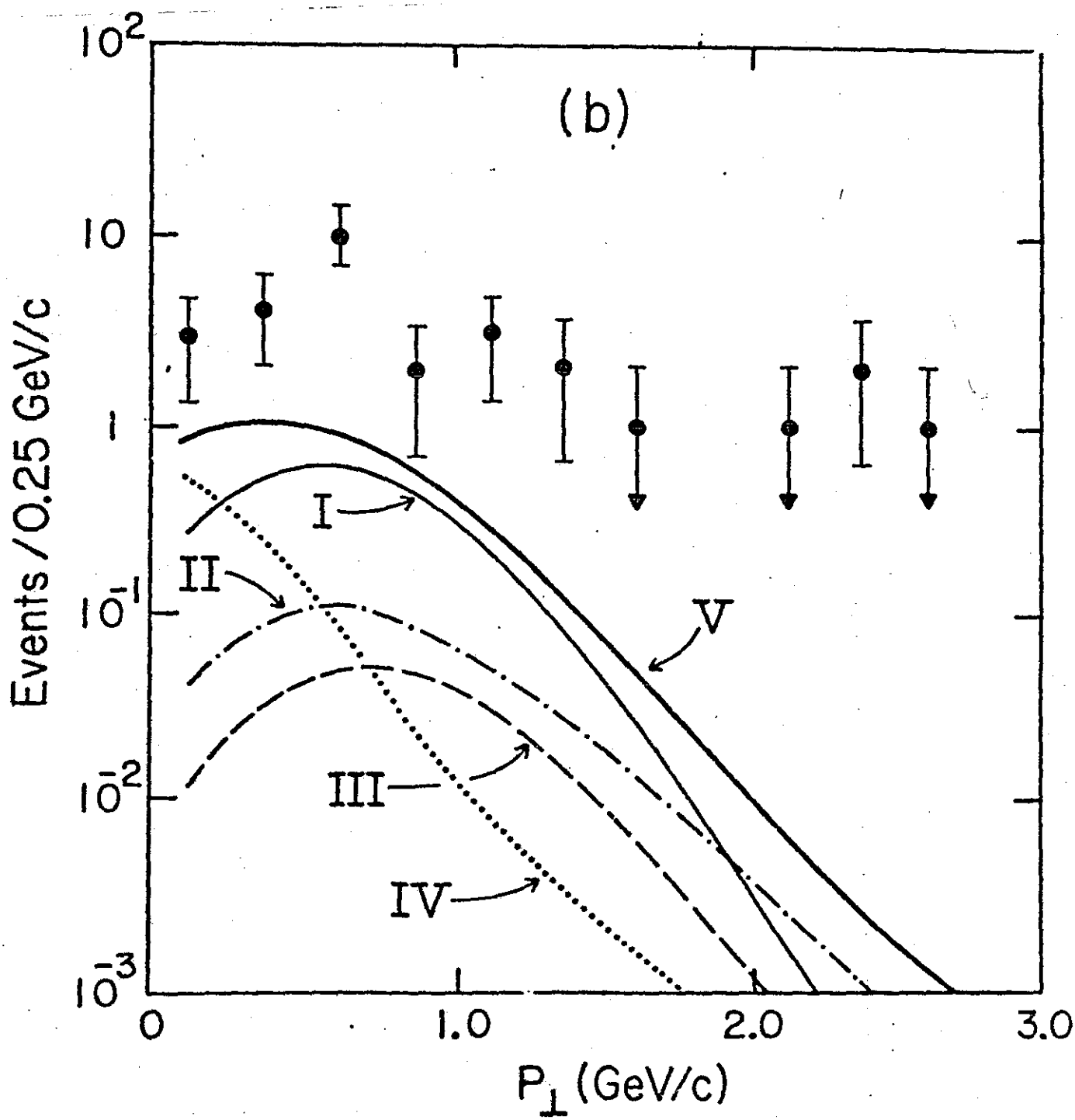
(b)
Events /0.25 GeV/c
10^2
10
1
10^{-1}
10^{-2}
10^{-3}
0
1.0
2.0
3.0
$P_\perp$ (GeV/c)
I
II
III
IV
V

FIGURE 4(b)